Nanoparticle optics: sensing with nanoparticle arrays and single nanoparticles

Richard P. Van Duyne, Amanda J. Haes, and Adam D. McFarland
*Department of Chemistry, Northwestern University, 2145 Sheridan Road, Evanston, IL USA 60208-3113

ABSTRACT

Recently, nanoparticles have become the platform for many sensing schemes. In particular, the utilization of the optical response of nanoparticles to changes in their nanoenvironment has served as a signal transduction mechanism for these sensing events. For example, silver nanoparticle arrays synthesized using nanosphere lithography have served as an ultrasensitive detection platform for small molecules, proteins, and antibodies with the detection limit of 60,000 and less than 25 molecules/nanoparticle for hexadecanethiol and antibodies, respectively. While this approach is low cost and highly portable, one limitation of the array platform is that the signal arises from approximately $1x10^6$ nanoparticles. A method to improve the overall number of molecules detected would be to decrease the number of nanoparticles probed. Recently, single nanoparticle sensing has been accomplished using dark-field microscopy. A 40 nm shift in the localized surface plasmon resonance induced from less than 60,000 small-molecule adsorbates has been monitored from a single Ag nanoparticle. Additionally, streptavidin sensing has also been demonstrated using a single Ag nanoparticle. Detection platforms based on nanoparticle arrays and single nanoparticles will be discussed and compared.

Keywords: Localized surface plasmon resonance, nanosphere lithography, nanoparticles, biosensors, streptavidin, alkanethiols, single nanoparticle sensing

1. INTRODUCTION

Metal nanoparticles have been used for hundreds of years to produce color in stained glass windows. Though scientists understood that different metal dispersions gave diverse characteristic hues, the advent of nanoscale analysis allowed them to understand how material properties such as metal, size, shape, and local dielectric environment affect the apparent color of a metal suspension. An understanding of the optical properties of noble metal nanoparticles holds both fundamental and practical significance. Fundamentally, it is important to systematically explore nanostructure characteristics that cause optical property variation as well as provide access to regimes of predictable behavior. Practically, the tunable optical properties of nanostructures can be applied as materials for surface-enhanced spectroscopy,[1, 2] optical filters,[3] plasmonic device,[4, 5] and sensors.[6-8] These nanoparticles exhibit a strong UV-vis absorption band that is not present in the spectrum of the bulk metal. This absorption band results when the incident photon frequency is resonant with the collective excitation of the conduction electrons and is known as the localized surface plasmon resonance (LSPR). LSPR excitation results in wavelength selective absorption with extremely large molar extinction coefficients ~ 3×10^{11} M^{-1} cm^{-1},[9-11] resonant Rayleigh[12, 13] scattering with an efficiency equivalent to that of 10^6 fluorophors, [14, 15]and the enhanced local electromagnetic fields near the surface of the nanoparticle which are responsible for the intense signals observed in all surface-enhanced spectroscopies.[16]

The simplest theoretical approach available for modeling the optical properties of nanoparticles is the Mie theory estimation of the extinction of a metallic sphere in the long wavelength, electrostatic dipole limit. In the following equation:[17]

* vanduyne@chem.northwestern.edu; phone 1 847 491-3516; fax 1 847 491-4530; www.chem.northwestern.edu/~vanduyne

$$E(\lambda) = \frac{24\pi N_A a^3 \varepsilon_m^{3/2}}{\lambda \cdot \ln(10)} \left[\frac{\varepsilon_i}{(\varepsilon_r + 2\varepsilon_m)^2 + \varepsilon_i^2} \right] \quad (1)$$

$E(\lambda)$ is the extinction (viz., sum of absorption and scattering), N_A is the areal density of nanoparticles, "a" is the radius of the metallic nanosphere, ε_m is the dielectric constant of the medium surrounding the metallic nanosphere (assumed to be a positive, real number and wavelength independent), λ is the wavelength of the absorbing radiation, ε_i is the imaginary portion of the metallic nanosphere's dielectric function, and ε_r is the real portion of the metallic nanosphere's dielectric function. Even in this most primitive model, it is abundantly clear that the LSPR spectrum of an isolated metallic nanosphere embedded in an external dielectric medium will depend on the nanoparticle radius "a", the nanoparticle material (ε_i and ε_r), and the nanoenvironment's dielectric constant (ε_m). Furthermore, when the nanoparticles are not spherical, as is always the case in real samples, the extinction spectrum will depend on the nanoparticle's in-plane diameter, out-of-plane height, and shape. The dependence of the extinction spectrum on these nanoparticle structural parameters has been recognized in the form of simplified model calculations such as those for ellipsoidal nanoparticle geometries.[10] In this case the denominator of the resonance term in equation 1.1 is replaced with:

$$(\varepsilon_r + \chi\varepsilon_m)^2 \quad (2)$$

where χ is a term that describes the nanoparticle aspect ratio. The values for χ increase from 2 (for a sphere) up to, and beyond, values of 17 for a 5:1 aspect ratio nanoparticle. In addition, many of the samples considered in this work contain an ensemble of nanoparticles that are supported on a substrate. Thus, the LSPR will also depend on interparticle spacing and substrate dielectric constant.

Nanosphere lithography (NSL) is a powerful fabrication technique to inexpensively produce nanoparticle arrays with controlled shape, size, and interparticle spacing.[18] The need for monodisperse, reproducible, and materials general nanoparticles has driven the development and refinement of the most basic NSL architecture as well as many new nanostructure derivatives. Every NSL structure begins with the self-assembly of size-monodisperse nanospheres of diameter D to form a two-dimensional colloidal crystal deposition mask. Methods for deposition of a nanosphere solution onto the desired substrate include spin coating,[18] drop coating,[19] and thermoelectrically-cooled angle coating.[20] All of these deposition methods require that the nanospheres be able to freely diffuse across the substrate seeking their lowest energy configuration. This is often achieved by chemically modifying the nanosphere surface with a negatively charged functional group such as carboxylate or sulfate that is electrostatically repelled by the negatively charged surface of a substrate such as mica or glass. As the solvent (water) evaporates, capillary forces draw the nanospheres together, and the nanospheres crystallize in a hexagonally close-packed pattern on the substrate. As in all naturally occurring crystals, nanosphere masks include a variety of defects that arise as a result of nanosphere polydispersity, site randomness, point defects (vacancies), line defects (slip dislocations), and polycrystalline domains. Typical defect-free domain sizes are in the 10 - 100 μm range. Following self-assembly of the nanosphere mask, a metal or other material is then deposited by thermal evaporation, electron beam deposition, or pulsed laser deposition from a collimated source normal to the substrate through the nanosphere mask to a controlled mass thickness, d_m. After metal deposition, the nanosphere mask is removed, typically by sonicating the entire sample in a solvent, leaving behind the material deposited through the nanosphere mask and onto the substrate.

In previous work, we reported a detailed study of the extreme sensitivity of the LSPR of triangular Ag nanoparticles.[6, 21-23] These Ag nanoparticles, with in-plane widths of 100 nm and out-of-plane heights of 50 nm, were fabricated using NSL. We demonstrated the following original features: 1) the refractive index sensitivity of nanoparticle arrays to bulk solvent is ~200 nm/RIU,[21] 2) the extinction maximum of the nanoparticles shifts 3 nm for every carbon atom in a monolayer for varying lengths of alkanethiols,[21] and 3) the extinction maximum, λ_{max}, of the LSPR shifts +27 nm for a complete monolayer coverage of streptavidin.[6] In these experiments, approximately $1x10^6$ nanoparticles are used to measure the nanosensor response. The detection limits of the system are less than 1 pM for streptavidin (<25 streptavidin molecules/nanoparticle)[6] and 10,000 molecules/nanoparticle for alkanethiols.[21]

Clearly, an obvious method to improve the limit of detection of the system would be to reduce the number of nanoparticles probed.[24]

A key to exploiting single nanoparticles as sensing platforms is to develop a technique to monitor the LSPR of individual nanoparticles with a reasonable signal-to-noise ratio. UV-visible absorption spectroscopy does not provide a practical means of accomplishing this task. Even under the most favorable experimental conditions, the absorbance of a single nanoparticle is very close to the shot noise-governed limit of detection. Instead, resonant Rayleigh scattering spectroscopy is the most straightforward means of characterizing the optical properties of individual metallic nanoparticles. Similar to fluorescence spectroscopy, the advantage of scattering spectroscopy lies in the fact that the scattering signal is being detected in the presence of a very low background. The instrumental approach for performing these experiments generally involves using high magnification microscopy coupled with oblique or evanescent illumination of the nanoparticles. Klar et al. utilized a near-field scanning optical microscope coupled to a tunable laser source to measure the scattering spectra of individual gold nanoparticles embedded in a TiO_2 film.[25] Sonnichsen et al. were able to measure the scattering spectra of individual electron beam lithography-fabricated nanoparticles using conventional light microscopy.[26] Their technique involved illuminating the nanoparticles with the evanescent field produced by total internal reflection of light in a glass prism. The light scattered by the nanoparticles was collected with a microscope objective and coupled into a spectrometer for analysis. Matsuo and Sasaki employed differential interference contrast microscopy to perform time-resolved laser scattering spectroscopy of single silver nanoparticles.[27] Mock et al. correlated conventional dark-field microscopy and TEM in order to investigate the relationship between the structure of individual metallic nanoparticles and their scattering spectra.[28] They have also used the same light microscopy techniques to study the response of the scattering spectrum to the particle's local dielectric environment by immersing the nanoparticle in oils of various refractive indexes.[29]

Recently, McFarland and Van Duyne demonstrated that single Ag nanoparticles can be used to sense local refractive index changes induced via bulk solvent changes and a monolayer of alkanethiols.[24] Specifically, using dark-field microscopy, the LSPR extinction maximum response of individual Ag nanoparticles to the adsorption of less than 60,000 hexadecanethiol molecules is ~40 nm. Additionally, kinetic responses were monitored and were found to be competitive with other real-time sensors.

This paper directly compares nanoparticle array and single nanoparticle sensing experiments. Experimental apparatus and procedures, alkanethiol sensitivity, and streptavidin sensitivity will be described and compared.

2. METHODOLOGY AND MATERIALS

2.1 Materials

1-Dodecanethiol and n-pentadecyl mercaptan were purchased from TCI (Portland, OR). 1-Tetradecanethiol was purchased from Fluka. 11-Mercaptoundecanoic acid (11-MUA), 1-Propanethiol, 1-butanethiol, 1-pentanethiol, 1-hexanethiol, 1-heptanethiol, 1-octanethiol (1-OT), 1-nonanethiol, 1-decanethiol, 1-dodecanethiol, hexadecanethiol, octadecyl mercaptan hexanes, and methanol were purchased from Aldrich (Milwaukee, WI). Anti-biotin, 1-ethyl-3-[3-dimethylaminopropyl]carbodiimide hydrochloride (EDC), streptavidin, 10 mM and 20 mM phosphate buffered saline (PBS) pH=7.4 was obtained from Sigma (St. Louis, MO). (+)-Biotinyl-3,6-dioxaoctanediamine (biotin) was purchased from Pierce (Rockford, IL). Absolute ethanol was purchased from Pharmco (Brookfield CT). Ag wire (99.95%, 0.5 mm) was purchased from D. F. Goldsmith (Evanston, IL). Borosilicate glass substrates were purchased from Fisher Scientific (Pittsburgh, PA). Polystyrene nanospheres with diameters of 400±7 nm (Interfacial Dynamics, Portland, OR) were received as a suspension in water. All materials were used without further purification.

2.2 Substrate Preparation

Glass substrates were cleaned in a piranha solution (1:3 30%H_2O_2:H_2SO_4) at 80°C for 30 minutes. Once cooled, the glass substrates were rinsed with copious amounts of water and then sonicated for 60 minutes in 5:1:1 H_2O:NH_4OH:30%H_2O_2. Next the glass was rinsed repeatedly with water and was stored in water until used.

2.3 Nanoparticle Array Preparation

NSL was used to fabricate monodisperse, surface-confined triangular Ag nanoparticles. A solution of nanospheres was drop coated onto a clean substrate and allowed to self-assemble into a 2D hexagonally close packed array that served as a deposition mask. On glass, single layer colloidal crystal nanosphere masks were prepared by drop coating ~2 μL of undiluted nanosphere solution on glass and mica substrates. The samples were then mounted into a Consolidated Vacuum Corporation vapor deposition chamber system. A Leybold Inficon XTM/2 quartz crystal microbalance (East Syracuse, NY) was used to monitor the thickness of the Ag film deposited on the nanosphere mask. All samples in this study were covered with 50.0 nm thickness Ag films. Following Ag vapor deposition, the nanosphere mask was removed by sonicating the samples in ethanol for 3 minutes.

2.4 Ultraviolet-visible Extinction Spectroscopy for Nanoparticle Arrays

Macroscale UV-visible extinction measurements were collected using an Ocean Optics spectrometer. All spectra collected are macroscopic measurements performed in standard transmission geometry with unpolarized light. The probe beam diameter was approximately 4 mm.

2.5 Experimental Setup and Nanoparticle Functionalization for Nanoparticle Arrays

A home-built flow cell was used to control the external environment of the Ag nanoparticle substrates (Figure 1A). Prior to modification, the Ag nanoparticles were solvent annealed with hexanes and methanol. Dry N_2 gas and solvent were cycled through the flow cell until the λ_{max} of the sample stabilized. Self-assembled monolayers (SAMs) were formed on the nanoparticles by incubation in a 3:1 ratio of 1 mM 1-OT:11-MUA in ethanol for 18-36 hours. Next, biotin was linked to the surface over a three hour time period via incubation in a 1:1 ratio of 1 mM EDC:biotin in 10 mM PBS. Samples were then incubated in 100 nM of streptavidin in PBS for three hours. Samples were rinsed thoroughly with 10 mM and 20 mM PBS after biotinylation and after detection of streptavidin to ensure removal of non-specifically bound materials.

2.6 Experimental Setup and Nanoparticle Functionalization for Single Nanoparticles

Colloidal Ag nanoparticles were prepared by reducing silver nitrate with sodium citrate in aqueous solution according to the procedure developed by Lee and Meisel.[30] These nanoparticles were immobilized by drop coating approximately 5 μL of the colloidal solution onto a no. 1 cover slip and allowing the water to evaporate. The cover slip was then inserted into a custom-designed flow cell. Prior to all experiments, the nanoparticles in the flow cell

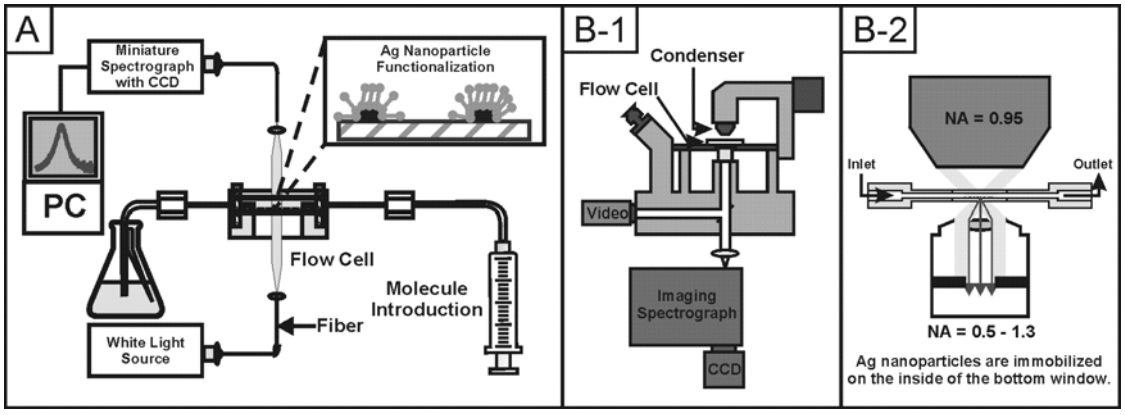

Figure 1. (A) Instrumental diagram for the array based LSPR nanosensor experiments. The flow cell is fiber optically coupled to a white light source and miniature spectrometer. The cell is linked directly to either a solvent reservoir or to a syringe containing the desired analyte. (B-1) Instrumental diagram used for single nanoparticle spectroscopy. (B-2) Close-up of the flow cell to show illumination and collection geometry.

were repeatedly rinsed with methanol and dried under nitrogen in order to establish equilibrium surface adsorption of solvent molecules and citrate anions. All optical measurements were performed using an inverted microscope (Eclipse TE300, Nikon Instruments) equipped with an imaging spectrograph (SpectroPro 300i, Roper Scientific) and a CCD detector (Spec-10:400B, Roper Scientific). A color video camera was also attached to the front port of the microscope to facilitate identification and alignment of the nanoparticles. The experimental apparatus is schematically depicted in Figure 1B. A dark-field condenser (NA=0.95) was used to illuminate the nanoparticles and a variable aperture 100X oil immersion objective (NA=0.5-1.3) was used to collect the light scattered by the nanoparticles.

Figure 2 illustrates the technique used to acquire the resonant Rayleigh scattering spectrum of single nanoparticles. First, the spectrometer grating was placed in zero order and the spectrometer entrance slit was opened to the maximum setting in order to project a wide-field image onto the CCD. Next, a nanoparticle was placed in the center of the field and the entrance slit was closed to 50 μm. Then the spectrometer grating (150 gr/mm) was rotated to disperse first-order diffracted light onto the CCD. To ensure that only the scattered light from a single nanoparticle was analyzed, the region of interest was selected using the CCD control software. An adjacent empty region of the CCD with the same dimensions was also collected in order to perform a background subtraction. Integration times varied depending on lamp intensity and the scattering strength of the nanoparticle, but a typical acquisition comprised of accumulating five exposures, each 15 seconds in duration. Finally, the raw scattering spectrum was normalized to correct for the lamp spectral profile, spectrometer throughput, and CCD efficiency. This was accomplished by dividing the raw spectrum by the lamp spectrum, which was obtained by increasing the numerical aperture of the objective above 0.95.

For streptavidin sensing, the nanoparticle was functionalized by incubating the sample in a 3:1 ratio of 1 mM 1-

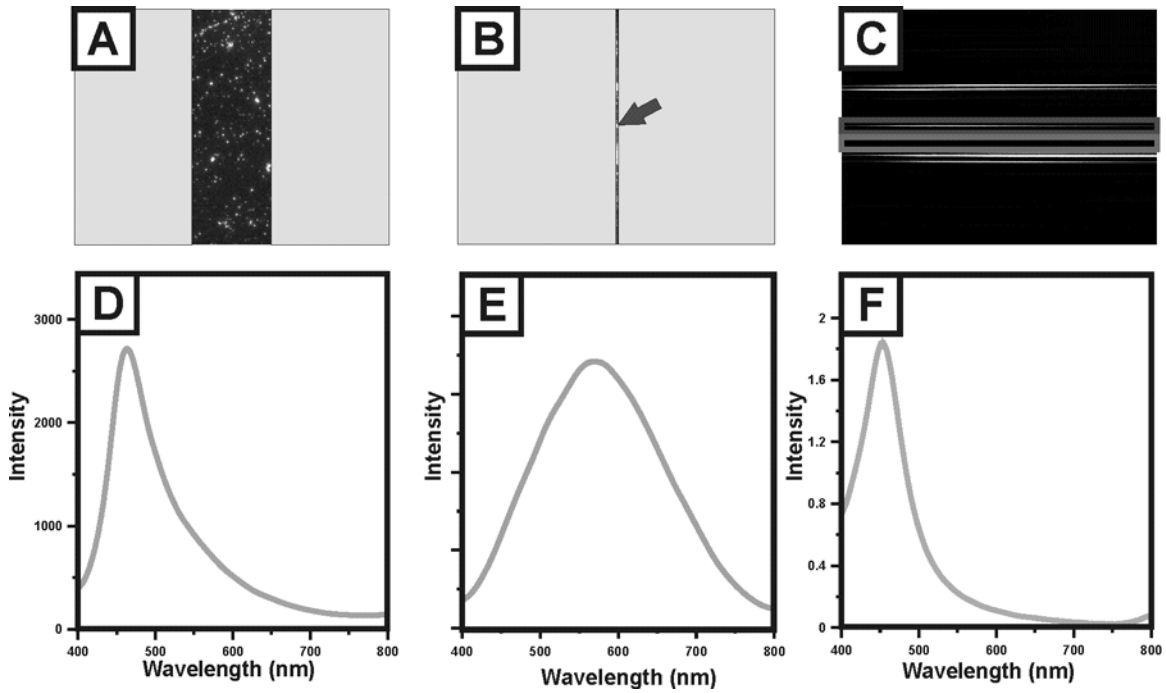

Figure 2. (A) Wide-field image of immobilized Ag nanoparticles. (B) A nanoparticle is centered and the entrance slit is closed to 50 μm. (C) The grating is rotated into a dispersion configuration and the regions of interest are selected [top box = nanoparticle spectrum, lower box=background]. (D) Raw scattering spectrum of a single Ag nanoparticle. (E) Lamp profile used for normalization of the scattering spectrum. (F) Normalized scattering spectrum with the LSPR λ_{max} = 452 nm.

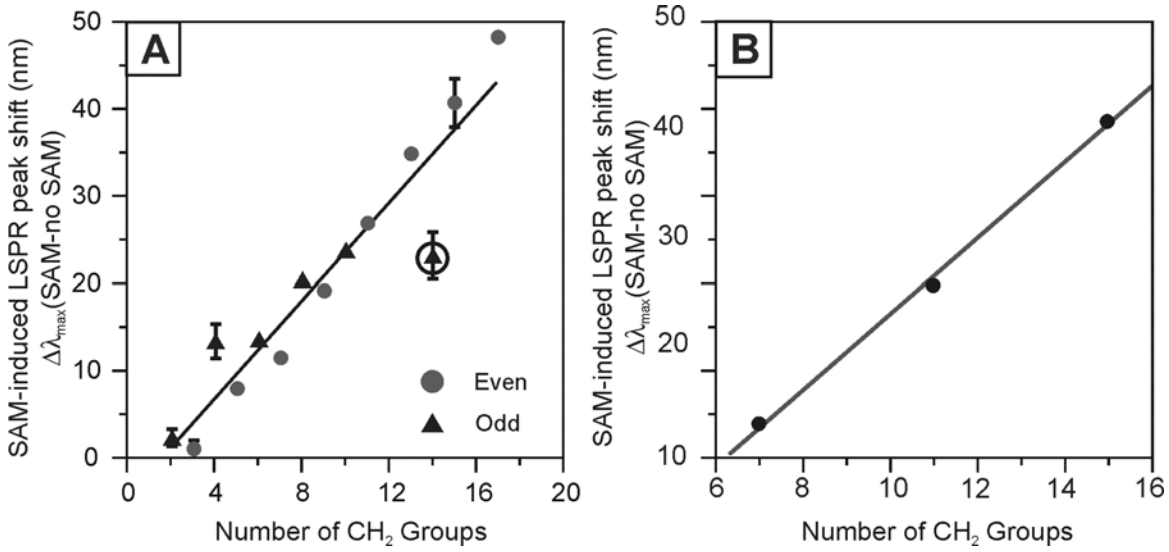

Figure 3. (A) Even and odd alkanethiol chain length dependence on the LSPR spectral peak shifts for Ag nanoparticles in arrays with in-plane widths = 100 nm and out-of-plane heights = 50.0 nm. All extinction measurements were collected in a nitrogen environment. Data points represent the averaged results. Error bars show the variation in the raw data. Linear regression was used to the line to the data described by the following equation: y= 3.06(x)-5.5. The circled point was not used when fitting the data. (B) Alkanethiol chain length dependence on a single Ag nanoparticle. Linear regression was used to fit the line to the data described by the following equation: y= 3.5(x)-12.0.

OT:11-MUA in ethanol for 18 hours. Next, biotin was covalently linked to the surface by incubation a 1:1 ratio of 1 mM EDC:biotin in 10 mM PBS for 18 hours. Resonant Rayleigh scattering spectra of an individual nanoparticle were collected before and after incubated in 10 nM streptavidin in PBS for two hours. Samples were rinsed thoroughly with 10 mM PBS after biotinylation and exposure to streptavidin to ensure removal of non-specifically bound materials.

3. RESULTS AND DISCUSSION

3.1 Effect of the Alkanethiol Chain Length on the LSPR for Ag Nanoparticle Arrays

For these studies, samples were incubated in 1.0 mM concentrations of the relevant alkanethiol ethanolic solution for 18-24 hours. Prior to incubation, the samples were solvent annealed and their stabilized extinction maxima were collected. The difference between the extinction maximum before and after incubation is the wavelength shift response reported. In all cases, each data point represents an average from a minimum of three separate samples.

Triangular silver nanoparticles have been shown to unexpectedly sensitive to alkanethiol adsorbates.[21, 31] For this study, the LSPR extinction maximum was compared before and after incubation in a given alkanethiol. For nanoparticles with in-plane widths of 100 nm and out-of-plane heights of 50.0 nm Ag, it shown that the LSPR extinction wavelength shifts 3.06 nm for every carbon atom in an adsorbed $CH_3(CH_3)_xSH$ monolayer for x=2-11, 13-15, and 17 (Figure 3A). Additionally, the y-intercept, which is related to the Ag-S charge transfer interaction, is -5.5 nm. Furthermore, it should be noted that these LSPR wavelength shifts are caused by only 60,000 alkanethiol molecules per nanoparticle.

3.2 Effect of the Alkanethiol Chain Length on the LSPR for Single Ag Nanoparticles

Just as in the nanoparticle arrays, the use of single nanoparticles as chemosensors was investigated using alkanethiol adsorbates. After recording the resonant Rayleigh scattering spectrum of an individual Ag nanoparticle in a N_2 environment, a 1.0 mM alkanethiol solution in ethanol was injected into the flow cell. The nanoparticles were

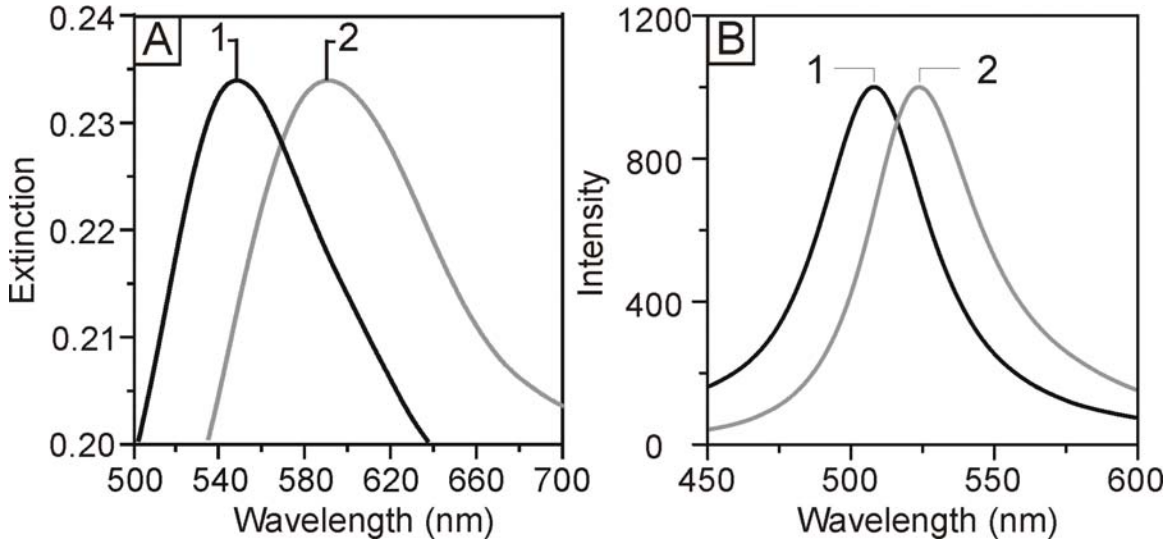

Figure 4. (A) LSPR spectra of the Ag nanoparticle array-based sensor illustrating the nanosensor's response to 100 nM streptavidin. All extinction measurements were collected in a nitrogen environment. (1) Biotinylated Ag nanoparticles, λ_{max}=609.6 nm. (2) After streptavidin incubation, λ_{max} =636.6 nm. (B) Individual Ag nanoparticle sensor before and after exposure to 10 nM streptavidin. All measurements were collected in a nitrogen environment. (1) Biotinylated Ag nanoparticle, λ_{max}=508.0 nm. (2) After streptavidin incubation, λ_{max} =520.7 nm.

incubated for at least one hour, even though real-time monitoring of scattering spectrum indicates that the majority of the response occurs in the first few minutes after injection. After incubation in the analyte solution, the flow cell was flushed several times with ethanol, methanol, and hexane in order to ensure that a maximum of one monolayer had adsorbed. Finally, the nanoparticle was dried under N_2 and a scattering spectrum was recorded.

Figure 3B shows the single nanoparticle LSPR λ_{max} response for the formation of three self assembled monolayers of various alkanethiol chain lengths. In an effort to ensure that Ag nanoparticles of similar size and shape were used, only nanoparticles exhibiting similar LSPR spectra and dielectric sensitivity were used. The observed response is linear with a sensitivity of +3.5 nm for each additional methylene group in the alkanethiol chain. Additionally, the y-intercept is -12 nm. These shifts are very similar to similar experiments performed on Ag nanoparticle arrays.

3.3 Streptavidin Sensing using Nanoparticle Arrays

The well-studied biotin-streptavidin system with its extremely high binding affinity (K_a~10^{13} M^{-1})[32] is chosen to illustrate the attributes of these LSPR-based nanoscale affinity biosensors. The biotin-streptavidin system has been studied in great detail by surface plasmon resonance spectroscopy[33, 34] and serves as an excellent model system for the LSPR nanosensor.[6] Streptavidin, a tetrameric protein, can bind up to four biotinylated molecules (i.e. antibodies, inhibitors, nucleic acids, etc.) with minimal impact on its biological activity[32] and, therefore, will provide a ready pathway for extending the analyte accessibility of the LSPR nanobiosensor.

NSL was used to create surface-confined triangular Ag nanoparticles supported on a glass substrate. The Ag nanotriangles have in-plane widths of ~ 100 nm and out-of-plane heights of ~ 51 nm as determined by AFM. The preparation of the LSPR nanosensor yields a 0.1 monolayer surface coverage of carboxylate binding sites. Since the maximum number of alkanethiol molecules per nanoparticle is 60 000, this is equivalent to ~ 6000 carboxylate binding sites per nanoparticle. Next, biotin was covalently attached to the carboxylate groups using a zero-length coupling reagent. The number of resulting biotin sites will be determined by the yield of this coupling reaction. Because this coupling is likely to be ~1-5% efficient, one expects there to be only 60-300 biotin sites per nanoparticle at maximum coverages.

Before surface functionalization, the Ag nanoparticles were exposed to solvent and N_2. In this study, the λ_{max} of the Ag nanoparticles were monitored during each surface functionalization step (Figure 4A). First, the LSPR λ_{max} of the bare Ag nanoparticles was measured to be 561.4 nm (not shown). To ensure a well-ordered SAM on the Ag nanoparticles, the sample was incubated in the thiol solution for 24 hours. After careful rinsing and thorough drying with N_2 gas, the LSPR λ_{max} after modification with the mixed SAM (not shown) was measured to be 598.6 nm. The LSPR λ_{max} shift corresponding to this surface functionalization step was a 38 nm red-shift, hereafter + will signify a red-shift and - a blue-shift, with respect to bare Ag nanoparticles. Next, biotin was covalently attached via amide bond formation with a two unit polyethylene glycol linker to carboxylated surface sites. The LSPR λ_{max} after biotin attachment (Figure 4A-1) was measured to be 609.6 nm corresponding to an additional + 11 nm shift. The LSPR nanosensor has now been prepared for exposure to the target analyte. Exposure to 100 nM streptavidin, resulted in LSPR λ_{max} = 636.6 nm (Figure 4A-2) corresponding to an additional +27 nm shift. It should be noted that the signal transduction mechanism in this nanosensor is a reliably measured wavelength shift rather than an intensity change as in many previously reported nanoparticle-based sensors.

3.2 Streptavidin Sensing with Single Nanoparticles

Streptavidin sensing has also been demonstrated on single Ag nanoparticles. After functionalization, the LSPR of an individual nanoparticle was measured to be 508.0 nm (Figure 4B-1). Next, 10 nM streptavidin was injected into the flow cell and the nanoparticle was allowed to incubate for 2 hours. Following this incubation and rinsing, the λ_{max} of the nanoparticle was measured at 520.7 nm (Figure 4B-2). This +12.7 nm shift arises from the detection of less than 700 streptavidin molecules. This response is estimated to arise from the detection of less than 700 streptavidin molecules.

During the course of our streptavidin experiments with single Ag nanoparticles, we became aware of a parallel research effort using Au nanoparticles and dark field microscopy.[35] The technique used by Rashke et al. involved functionalizing spherical Au nanoparticles with biotinylated bovine serum albumin (BSA) and monitoring the LSPR shift of a single nanoparticle during exposure to 2 μM streptavidin. The maximum LSPR shift that they observed was approximately +1.2 nm. This relatively small response is a consequence of four aspects of their experimental conditions: (1) all spectra were recorded while the nanoparticle was immersed in a buffer solution, (2) the binding of streptavidin inside the BSA layer causes very little change in the local dielectric environment of the nanoparticle (3) the dielectric sensitivity of Au nanoparticles is smaller than Ag nanoparticles of equivalent geometry,[36] and (4) spherical nanoparticles exhibit the lowest dielectric sensitivity ($\chi = 2$). The +12.7 nm response demonstrated in our work is a result of the following advantages of our experimental conditions: (1) all spectra were recorded while the nanoparticle was immersed in N_2, (2) the SAM functionalization dictates that streptavidin binding causes a significant change in the local dielectric environment of the nanoparticle, (3) a Ag nanoparticle was used, and (4) the nanoparticle geometry was most likely a disk or platelet ($\chi >> 2$) based on analysis of its LSPR spectrum and similar assignments made by Mock et al.[29] Because the LSPR response of nanoparticle is ultimately a function of the change in local refractive index, performing our experiment in PBS (refractive index (RI) = 1.33) as opposed to N_2 (RI = 1.00) would result in an estimated 58% decrease in response. Therefore, saturation coverage of streptavidin (RI = 1.57) would result in a +5.3 nm response even with the nanoparticle continuously immersed in PBS.

4. CONCLUSIONS

This work summarizes our advances made in the area of nanoparticle-based sensors. Ag nanoparticle arrays provide a low-cost, high-throughput screening method for the sensing of both small molecules and proteins with a very low limit of detection. This was demonstrated via the detection of varying lengths of alkanethiols and streptavidin. The extension of LSPR sensing technique to the single nanoparticle limit provides several improvements over existing array- or cluster-based techniques. First, absolute detection limits are dramatically reduced. The surface area of chemically prepared Ag nanoparticles is typically less than 20,000 nm^2, which requires that a complete monolayer of adsorbate must constitute fewer than approximately 100 zeptomole. As demonstrated above, the formation of alkanethiol monolayers on Ag nanoparticles can result in a LSPR λ_{max} shift of greater that 40 nm, a change that is over 100 times larger than the resolution of convention UV-visible spectrometers. This suggests that the limit of detection for single nanoparticle-based LSPR sensing will be well below 1,000 molecules for small molecule

adsorbates. For larger molecules such as antibodies and proteins that result a greater change in the local dielectric environment upon surface adsorption, the single molecule detection limit may be achieved. Second, the extreme sensitivity of single nanoparticle sensors dictates that only very small sample volumes (viz., attoliters) are necessary to induce a measurable response. This characteristic would eliminate the need for analyte amplification techniques (e.g., polymerase chain reaction) required by other analytical methods. Third, single nanoparticle sensing platforms are readily applicable to multiplexed detection schemes. By controlling the size, shape, and chemical modification of individual nanoparticles, multiple sensing platforms can be generated in which each unique nanoparticle can be distinguished from the others based on the spectral location of its LSPR. Several of these unique nanoparticles can then be incorporated into a one device, allowing for the rapid, simultaneous detection of thousands of different chemical or biological species.

This paper highlights representative research accomplishments in the area of fundamental and applied studies of the tunable LSPR. Specific applications in the Van Duyne laboratory include exploitation of the LSPR as a signal transduction mechanism for sensing applications and optimization of SERS signals. The optical properties of metallic nanostructures will find future application in the areas of dichroic filters, plasmonic waveguides, data storage, biological labels and sensors. Commercialization of nanoparticle devices relies on better understanding of the electromagnetic interaction between nanoparticles as well as the development of techniques that will preserve nanoparticle optical activity in adverse environments.

ACKNOWLEDGEMENTS

We acknowledge support of the Nanoscale Science and Engineering Initiative of the National Science Foundation under NSF Award Number EEC-0118025. Any opinions, findings and conclusions or recommendations expressed in this material are those of the authors and do not necessarily reflect those of the National Science Foundation. A. J. Haes also wishes to acknowledge the American Chemical Society Division of Analytical Chemistry and Dupont for a graduate fellowship. The authors also acknowledge support from the American Chemical Society Petroleum Research Fund (PRF#37982-ACS).

REFERENCES

1. R. G. Freeman, K. C. Grabar, K. J. Allison, R. M. Bright, J. A. Davis, A. P. Guthrie, M. B. Hommer, M. A. Jackson, P. C. Smith, D. G. Walter and M. J. Natan, "Self-Assembled Metal Colloid Monolayers: An Approach to SERS Substrates," *Science* **267**, pp. 1629-1632, 1995.
2. M. Kahl, E. Voges, S. Kostrewa, C. Viets and W. Hill, "Periodically structured metallic substrates for SERS," *Sens. Actuator B-Chem.* **51**, pp. 285-291, 1998.
3. Y. Dirix, C. Bastiaansen, W. Caseri and P. Smith, "Oriented Pearl-Necklace Arrays of Metallic Nanoparticles in Polymers: A New Route Toward Polarization-Dependent Color Filters," *Adv. Mat.* **11**, pp. 223-227, 1999.
4. S. A. Maier, M. L. Brongersma, P. G. Kik, S. Meltzer, A. A. G. Requicha and H. A. Atwater, "Plasmonics-A Route to Nanoscale Optical Devices," *Adv. Mat.* **13**, pp. 1501-1505, 2001.
5. S. A. Maier, P. G. Kik, H. A. Atwater, S. Meltzer, E. Harel, B. E. Koel and A. A. G. Requicha, "Local detection of electromagnetic energy transport below the diffraction limit in metal nanoparticle plasmon waveguides," *Nat. Mat.* **2**, pp. 229-232, 2003.
6. A. J. Haes and R. P. Van Duyne, "A Nanoscale Optical Biosensor: Sensitivity and Selectivity of an Approach Based on the Localized Surface Plasmon Resonance Spectroscopy of Triangular Silver Nanoparticles," *J. Am. Chem. Soc.* **124**, pp. 10596 - 10604, 2002.
7. R. C. Mucic, J. J. Storhoff, C. A. Mirkin and R. L. Letsinger, "DNA-Directed Synthesis of Binary Nanoparticle Network Materials," *J. Am. Chem. Soc.* **120**, pp. 12674-12675, 1998.
8. L. R. Hirsch, J. B. Jackson, A. Lee, N. J. Halas and J. L. West, "A Whole Blood Immunoassay Using Gold Nanoshells," *Anal. Chem.* **75**, pp. 2377-2381, 2003.
9. T. R. Jensen, M. D. Malinsky, C. L. Haynes and R. P. Van Duyne, "Nanosphere Lithography: Tunable Localized Surface Plasmon Resonance Spectra of Silver Nanoparticles," *J. Phys. Chem. B* **104**, pp. 10549-10556, 2000.
10. S. Link and M. A. El-Sayed, "Spectral Properties and Relaxation Dynamics of Surface Plasmon Electronic Oscillations in Gold and Silver Nano-dots and Nano-rods.," *J. Phys. Chem. B* **103**, pp. 8410-8426, 1999.

11. M. A. El-Sayed, "Some Interesting Properties of Metals Confined in Time and Nanometer Space of Different Shapes.," *Acc. Chem. Res.* **34**, pp. 257-264, 2001.
12. A. M. Michaels, M. Nirmal and L. E. Brus, "Surface Enhanced Raman Spectroscopy of Individual Rhodamine 6G Molecules on Large Ag Nanocrystals.," *J. Am. Chem. Soc.* **121**, pp. 9932-9939, 1999.
13. S. Schultz, D. R. Smith, J. J. Mock and D. A. Schultz, "Single-target molecule detection with nonbleaching multicolor optical immunolabels," *P.N.A.S.* **97**, pp. 996-1001, 2000.
14. J. Yguerabide and E. E. Yguerabide, "Light-scattering submicroscopic particles as highly fluorescent analogs and their use as tracer labels in clinical and biological applications - I. Theory," *Anal. Biochem.* **262**, pp. 137-156, 1998.
15. J. Yguerabide and E. E. Yguerabide, "Light-scattering submicroscopic particles as highly fluorescent analogs and their use as tracer labels in clinical and biological applications - II. Experimental characterization," *Anal. Biochem.* **262**, pp. 157-176, 1998.
16. G. C. Schatz and R. P. Van Duyne, *Electromagnetic Mechanism of Surface-Enhanced Spectroscopy*, Wiley, New York, 2002.
17. U. Kreibig and M. Vollmer, *Cluster Materials*, Springer-Verlag, Heidelberg, Germany, 1995.
18. J. C. Hulteen and R. P. Van Duyne, "Nanosphere Lithography: A Materials General Fabrication Process for Periodic Particle Array Surfaces," *J. Vac. Sci. Technol. A* **13**, pp. 1553-1558, 1995.
19. J. C. Hulteen, D. A. Treichel, M. T. Smith, M. L. Duval, T. R. Jensen and R. P. Van Duyne, "Nanosphere Lithography: Size-Tunable Silver Nanoparticle and Surface Cluster Arrays," *J. Phys. Chem. B* **103**, pp. 3854-3863, 1999.
20. R. Micheletto, H. Fukuda and M. Ohtsu, "A Simple Method for the Production of a Two-Dimensional, Ordered Array of Small Latex Particles," *Langmuir* **11**, pp. 3333-3336, 1995.
21. M. D. Malinsky, K. L. Kelly, G. C. Schatz and R. P. Van Duyne, "Chain Length Dependence and Sensing Capabilities of the Localized Surface Plasmon Resonance of Silver Nanoparticles Chemically Modified with Alkanethiol Self-Assembled Monolayers," *J. Am. Chem. Soc.* **123**, pp. 1471-1482, 2001.
22. A. J. Haes and R. P. Van Duyne, "A Highly Sensitive and Selective Surface-Enhanced Nanobiosensor," *Mat. Res. Soc. Symp. Proc.* **723**, pp. O3.1.1-O3.1.6, 2002.
23. J. C. Riboh, A. J. Haes, A. D. McFarland, C. R. Yonzon and R. P. Van Duyne, "A Nanoscale Optical Biosensor: Real-Time Immunoassay in Physiological Buffer Enabled by Improved Nanoparticle Adhesion," *J. Phys. Chem. B* **107**, pp. 1772-1780, 2003.
24. A. D. McFarland and R. P. Van Duyne, "Single Silver Nanoparticles as Real-Time Optical Sensors with Zeptomole Sensitivity," *Nano Letters* pp. ASAP, 2003.
25. T. Klar, M. Perner, S. Grosse, G. von Plessen, W. Spirkl and J. Feldmann, "Surface-Plasmon Resonances in Single Metallic Nanoparticles," *Physical Review Letters* **80**, pp. 4249-4252, 1998.
26. C. Sonnichsen, S. Geier, N. E. Hecker, G. von Plessen, J. Feldmann, H. Ditlbacher, B. Lamprecht, J. R. Krenn, F. R. Aussenegg, V. Z.-H. Chan, J. P. Spatz and M. Moller, "Spectroscopy of single metallic nanoparticles using total internal reflection microscopy," *Appl. Phys. Lett.* **77**, pp. 2949-2951, 2000.
27. Y. Matsuo and K. Sasaki, "Time-Resolved Laser Scattering Spectroscopy of a Single Metallic Nanoparticle," *Jpn. J. Appl. Phys.* **40**, pp. 6143-6147, 2001.
28. J. J. Mock, S. J. Oldenburg, D. R. Smith, D. A. Schultz and S. Schultz, "Composite Plasmon Resonant Nanowires," *Nano Letters* **2**, pp. Web Release Date: 20-Apr, 2002.
29. J. J. Mock, D. R. Smith and S. Schultz, "Local Refractive Index Dependence of Plasmon Resonance Spectra from Individual Nanoparticles," *Nano Letters* **3**, pp. 485-491, 2003.
30. P. C. Lee and D. Meisel, "Adsorption and Surface-Enhanced Raman of Dyes on Silver and Gold Sols," *J. Phys. Chem.* **86**, pp. 3391-3395, 1982.
31. A. J. Haes, S. Zou, G. C. Schatz and R. P. Van Duyne, "A Nanoscale Optical Biosensor: The Short Range Distance Dependence of the Localized Surface Plasmon Resonance of Noble Metal Nanoparticles," *in preparation* pp. 2003.
32. N. M. Green, "Avidin," *Adv. Proten Chem.* **29**, pp. 85-133, 1975.
33. L. S. Jung and C. T. Campbell, "Sticking Probabilities in Adsorption of Alkanethiols from Liquid Ethanol Solution onto Gold.," *J. Phys. Chem. B* **104**, pp. 11168-11178, 2000.
34. V. H. Perez-Luna, M. J. O'Brien, K. A. Opperman, P. D. Hampton, G. P. Lopez, L. A. Klumb and P. S. Stayton, "Molecular Recognition between Genetically Engineered Streptavidin and Surface-Bound Biotin.," *J. Am. Chem. Soc.* **121**, pp. 6469-6478, 1999.

35. G. Raschke, S. Kowarik, T. Franzl, C. Sonnichsen, T. A. Klar and J. Feldmann, "Biomolecular Recognition Based on Single Gold Nanoparticle Light Scattering," *Nano Letters* pp. ASAP, 2003.
36. E. D. Palik, *Handbook of Optical Constants of Solids*, Academic Press, Inc., New York, 1985.